Peptide Crystallization

DOI: 10.1002/anie.201103941

Uniaxially Oriented Peptide Crystals for Active Optical Waveguiding**

Xuehai Yan, Ying Su, Junbai Li,* Johannes Früh, and Helmuth Möhwald*

Oriented organization or crystallization is ubiquitous in biological systems such as filamentous viruses,[1] membrane proteins (e.g. proteorhodopsin),[2] annulus fibrosus,[3] and actin filaments.[4] Inspired by the elegant biological world, researchers can delicately manipulate a wide range of biological and synthetic building blocks into ordered superstructures with precisely controlled dimensions by using a bottom-up self-assembly approach.[5] Biomimetic or bioinspired functional materials with ordered organization at the micrometer or nanometer scale, fabricated from peptide building blocks, are of increasing interest owing to their structural simplicity, functional versatility, cost efficiency, and biocompatibility.[5b,6] However, a significant challenge remains to create and develop such complex functional materials with multiple ordered structures by low-cost solution-phase protocols.[7,8] If these structures could be constructed from biological or bioinspired molecules, they would be very flexible, lightweight, responsive, and biocompatible and degradable for use in biological systems.

We report herein the first observation of three-dimensional (3D) oriented crystallization that produces long-range order in a self-assembling fibrous peptide network. The crystallization can be readily triggered by the introduction of an aldehyde into the fibrous networks (Scheme 1). The precise structural definition achieved in the process of crystallization enables collective organization into clusters or arrays, which results in the appearance of periodic ordered structures in the 3D macroscopic assemblies. The anisotropic peptide fibers that are confined in the crystalline platelets are uniaxially oriented along the long axis, reminiscent of the fiber grain in wood. Surprisingly, the resultant peptide crystal can act as an active optical waveguide that allows photoluminescence (PL) propagation along its long axis. To our knowledge, this is the first observation of optical waveguiding in a single-crystalline peptide structure. Such systems would greatly expand the use of waveguide materials[9–12] into a broader range of biological or biomedical fields in which biocompatible and biodegradable properties are highly appreciated. This finding opens up a new, cost-effective way to engineer optical materials from biological or biologically derived small molecules with simple chemical structures.

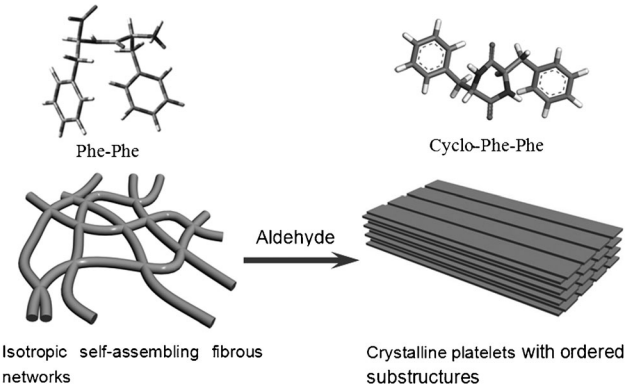

Scheme 1. Schematic illustration of oriented crystallization at long range in self-assembling fibrous peptide networks. Crystallization is triggered by introduction of an aldehyde. The resulting crystalline platelet consists of cyclo-Phe-Phe, a cyclization product of diphenylalanine (FF).

Crystallization was studied starting from a gel fibrous network of diphenylalanine (L-Phe-L-Phe, FF), which was inspired by the pathogenic process of Alzheimer's disease.[13] Analogously to the reported method,[14] peptide gel was first prepared by using 0.4 M FF solution in 1,1,1,3,3,3-hexafluoro-2-propanol (HFP, 20 μL) to gelate toluene solution of an aldehyde (0.5 mL). Such a peptide gel with trapped aldehyde was then allowed to age for a period of one month. It was found that gel networks collapsed gradually, yielding a white precipitate. Scanning electron microscopy (SEM) images (Figure S1a in the Supporting Information) show that the precipitate consists of rectangular platelets with dimensions with over tens of micrometers (up to 500 μm) in length, ten or more micrometers in width, and hundreds of nanometers in height. The magnified SEM image (Figure 1a) of a single platelet reveals anisotropic peptide fiber or ribbon structures which are confined in the crystalline platelet and uniaxially oriented along the longitudinal axis, reminiscent of the fiber grain in wood. Transmission electron microscopy (TEM, Figure S1b) reveals a regular platelet which is grown from self-assembling peptide fibrous networks. The TEM image of the broken edge of a single platelet exhibits details of the morphology inside. It reveals that the platelet consists of

[*] Dr. X. Yan, J. Früh, Prof. Dr. Dr. H. Möhwald
Max Planck Institute of Colloids and Interfaces
Am Mühlenberg 1, 14476 Potsdam/Golm (Germany)
E-mail: xuehai.yan@mpikg.mpg.de
Y. Su, Prof. Dr. J. Li
Beijing National Laboratory for Molecular Sciences (BNLMS)
Key Lab of Colloid and Interface Sciences
Institute of Chemistry, Chinese Academy of Sciences
Beijing 100190 (China)
E-mail: jbli@iccas.ac.cn

[**] X.Y. acknowledges support for a research fellowship from the Alexander von Humboldt Foundation. We acknowledge the financial support of this research by the National Basic Research Program of China (973 program) 2009CB30101 and the Chinese Academy of Sciences as well as the German Max Planck Society. X.Y. thanks H. Runge, R. Pitschke, and A. Heilig for technical assistance as well as H. Zhang for great help in molecular modeling. Dr. P. Zhu is thanked for helpful discussion. Prof. J. Zhai, K. F. Wang, and W. Cui are thanked for their kind help in SNOM measurement.

Supporting information for this article is available on the WWW under http://dx.doi.org/10.1002/anie.201103941.

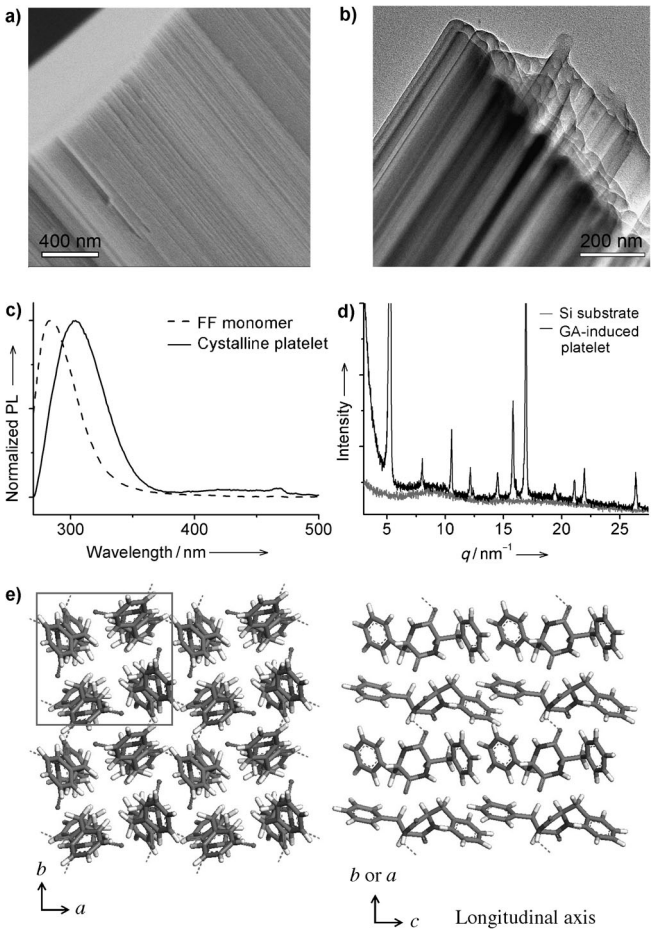

Figure 1. a) Magnified SEM image and b) magnified TEM image of a single crystalline platelet. c) Fluorescence spectra of FF monomer in HFP solution and crystalline platelet on quartz substrate. d) XRD pattern of glutaraldehyde (GA)-induced platelets on a silicon substrate. e) Molecular organization based on the refinement of XRD data and molecular simulation. For the view along the *c* axis (left), the hydrogen bonding pattern can be clearly observed. The image provides a detailed view of aromatic interactions between peptide molecules.

directionally aligned ribbons with 3D layered stacking (Figure 1b). The selected-area electron diffraction (SAED) pattern (Figure S2 in the Supporting Information) of a representative peptide platelet reveals that the peptide platelet is single-crystalline. In tapping-mode atomic force microscopy (AFM), the 3D height image (Figure S1c in the Supporting Information) clearly indicates the spatial dimensions of the platelet with thickness 300 nm. The scanning on the surface of such a platelet confirms the presence of anisotropic fiber or ribbon texture (Figure S1d in the Supporting Information), in agreement with the observation in SEM inspection. All in all, the microscopic characterization indicates that the well-defined platelet organized with 3D ordered anisotropic subunits is easily accessible merely by introduction of an aldehyde into self-assembling fibrous networks.

The chemical structure of the crystalline platelets was identified by matrix-assisted laser desorption/ionization time-of-flight (MALDI-TOF) mass spectrometry and NMR spectroscopy. As shown in the mass spectrum of FF powder, there are three characteristic peaks at 313, 335, and 351 m/z (mass to charge ratio) indicative of $M\mathrm{H}^+$, $M\mathrm{Na}^+$, and $M\mathrm{K}^+$ of the FF molecule (Figure S3a in the Supporting Information; see also molecular structure (top left in Scheme 1)), respectively. In comparison, the emergence of three new characteristic peaks at 295, 317, and 333 m/z indicates an alteration of the chemical structure in the formation of crystalline platelets. These new MS peaks can be assigned to $M\mathrm{H}^+$, $M\mathrm{Na}^+$, and $M\mathrm{K}^+$ of cyclo-Phe-Phe (CPP, Figure S3bc in the Supporting Information; see also the molecular structure (top right in Scheme 1)), a cyclization product of FF. ^{1}H NMR spectra of FF powder and crystalline platelets show significant differences, which imply a change in the chemical structure before and after crystallization (Figure S4 in the Supporting Information). The NMR spectrum of crystalline platelets is exclusively correlated with cyclo-Phe-Phe. It has been reported that the cyclization of dipeptides in toluene could be triggered by elevating the temperature for reflux or by induction with a small amount of acid or base at room temperature.[15] In our case, the cyclization is performed at room temperature and occurs exclusively upon introduction of an aldehyde. It is thus conjectured that the Schiff's reaction between the aldehyde group and the primary amine of FF peptide produces a small amount of Schiff's base, which then triggers the cyclization reaction. In a control experiment in which FF gel in toluene was aged for over one month, we did not observe any disassembly and the appearance of precipitates. This finding also indirectly confirms the decisive role of the aldehyde in triggering the cyclization of dipeptide at room temperature. Taken together, the results indicate that the linear FF peptide undergoes backbone cyclization upon the introduction of aldehyde into self-assembling fibrous networks, which thus gives rise to crystallization and eventually leads to the formation of ordered crystalline platelets composed of CPP.

FTIR spectra of the assemblies before and after crystallization reveal remarkable diversity (Figure S5 in the Supporting Information). The β-sheet signal in FF fibrils, assigned on the basis of the position of the amide I band at 1620 and 1683 cm^{-1}, disappears after crystallization. Instead, one new peak arises at 1676 cm^{-1} corresponding to a possible β-turn secondary structure in the crystalline platelet.[16] The other peak at 1660 cm^{-1} in the amide I band is associated with the free-stretching C=O vibration, namely the non-hydrogen-bonded amide carbonyl group.[16] This result implies that not all carbonyl groups are involved in the formation of hydrogen bonding, consistent with the result of molecular simulations (see below). The obvious downshift of the amide A band from 3274 cm^{-1} in FF fibrils to 3204 cm^{-1} in CPP crystalline platelets indicates the possible enhancement of hydrogen-bonding interactions of the NH group after crystallization.[16] Photoluminescence (PL) spectra of FF monomers in HFP and of crystalline platelets are shown in Figure 1c. The phenyl groups in the FF monomer have an emission peak at 284 nm, characteristic of the phenylalanine residue,[17] which shifts to 303 nm for the crystals. The red shift suggests an effective π–π stacking between the aromatic residues of CPP peptide, which

is regarded as another possible driving force for the formation of crystalline platelets.

Insight into the structure of crystalline platelets is obtained by X-ray diffraction (XRD) measurements and polarized optical microscopy. The XRD pattern of platelets confirms their crystalline nature, as evidenced by the intense sharp Bragg peaks (Figure 1 d and Figure S6a in the Supporting Information). The indexing of the XRD pattern reveals that the peptide crystal possibly has a tetragonal lattice, the structural parameters of which are provided in Table S1. Pawley and Rietveld refinements were performed to optimize the lattice parameters. Molecular packing in crystalline platelets is shown in Figure 1 e. The lattice consists of four peptide molecules and is held together by the combination of hydrogen bonds and aromatic stacking (Figure 1 e), which lend overall stability to the crystalline structure. The aromatic stacking appears to play a decisive role for the formation of elongated chains along the *c* axis (Right image in Figure 1 e). The peptide backbone is oriented along the fast growth axis, the *c* axis, or the confined anisotropic ribbon long axis. From this molecular packing model, it can be also deduced that only one carbonyl group for each peptide molecule participates in the formation of hydrogen bonds, which mirrors the result of the FTIR spectrum. The crystals obtained by introducing either glutaraldehyde (GA) or formaldehyde (FA) exhibit essentially identical same XRD patterns (Figure S6a in the Supporting Information). Slight differences in intensity of XRD patterns and the relative intensity of the peak of ionized fragments detected from MS analysis (Figure S3b,c in the Supporting Information) is ascribed to differences in molecular organization and strengths of intermolecular forces, which possibly result from different crystallization rates undergoing dynamic regulation in the process of crystal growth. Figure S6b in the Supporting Information shows images of crystalline platelets under crossed polarizers. It can be seen that some of the platelets are very dark under crossed polarizers (Left image in Figure S6b in the Supporting Information), which implies that their optical axis is oriented parallel to the direction of the objective polarizer, which thus leads to light extinction. Rotating the relative orientation between sample and polarizers by 45°, the dark platelets turn to be bright, whereas some originally bright platelets become dark (right image in Figure S6b in the Supporting Information). Such optical changes indicate that cyclo-Phe-Phe molecules are uniaxially oriented (likely along their long axis, the *c* axis) within the crystalline platelet, thus leading to strong anisotropy of the refractive index.[18]

The growth process of crystalline platelets was studied in detail by monitoring the self-assembling gel networks with time (Figure S7 in the Supporting Information). At the beginning (aging for one day), some of the self-assembling FF fibrils were cross-linked to form spherical structures as a result of the Schiff's base reaction between the aldehyde group and the terminal NH_2 group in FF molecules. After the system has aged for two days, we can clearly observe the appearance of thin crystalline flakes with leaf-like shape. In association with the composition of crystalline platelets as confirmed above, it is ensured that the cyclization of linear FF dipeptide has taken place. With the increase of ageing time, more CPP can be produced, which results in the formation of more crystalline flakes. After ten days, a regular platelet with lamellar stacking could be observed, which resulted from further growth. Subsequently, more and bigger platelets were found, but most of them existed in a sawtoothed form. Actually, at this stage a colorful supernatant including cross-linked spheres appeared, and white precipitate was observed at the bottom. The crystalline platelets with clear spatial dimensions could be obtained after 30 days of ageing (Figure S7f in the Supporting Information). The magnified SEM image showed the hierarchical organization of platelets and orientation of substructures in the crystal. It is thus speculated that the crystallization in self-assembling fibrous networks is connected to the mechanism of nucleation and growth, for which the monomers offered for crystallization are generated stepwise by the cyclization of linear FF peptides. The crystalline flakes seen in the initial stage of crystallization show no obvious substructures (that is, the confined ribbon structures as observed in the final platelets). This finding indicates that the confinement of anisotropic ribbon structures in crystalline platelets likely results from automatic adjustment in the process of crystal growth. As reported, crystallization of systems with embedded ordered nanostructures is generally regarded as a result of kinetic control in nucleation and growth.[19] In the present case, the cyclic dipeptide crystallization is presumably subject to kinetic regulation, which proceeds by a sequential process of structural modifications of crystalline intermediates rather than by a single-step pathway.[19]

To determine the effect of aldehyde concentration on the crystallization, experiments were performed with different amounts of aldehyde. As shown in Figure S8 in the Supporting Information, the gel color gradually darkens with increasing GA content. The color results from the Schiff's bases formed between FF and GA. Deeper color implies higher Schiff's base yield. However, addition of excessive GA (e.g., 0.06 M GA toluene solution) prevents gel formation, because the reaction between GA and FF consumes a number of FF molecules responsible for gel formation. It is found that the introduction of more GA results in faster formation of peptide platelets, but that the total weight is less (Table S2 in the Supporting Information). The results indicate that more aldehyde is more reactive and leads to the production of more Schiff's bases, thus speeding up the kinetics of the reaction for CPP formation and subsequent crystallization. Also, more aldehyde facilitates the phase transition from gel states to crystals by destabilizing the gel network. On the one hand, this is because more aldehyde leads to the formation of more cross-linked spherical structures (Figure S7a in the Supporting Information), which weakens the gel strength. On the other hand, production and subsequent crystallization of CPP separately by digestion of the FF initiates the phase isolation.

The gel state plays a key role in determining the structures of the final crystals. Confined organization of periodic substructures in the resulting crystals is presumably the result of the relatively slow crystallization process. This assumption is supported by comparison with a rapid crystallization process in which CPP was directly assembled in bulk solution. When CPP (2 mg) was first dissolved in HFP

(100 μL) and then diluted to a final concentration of 4 mg mL^{-1} with toluene, flowerlike superstructures were observed within a few minutes by optical microscopy (Figure S9a in the Supporting Information), thus indicating that CPP molecules undergo rapid self-assembly in this case. SEM images further confirm the formation of flowerlike aggregates by CPP self-assembly (Figure S9b in the Supporting Information). The magnified SEM image indicates that the aggregates consist of short and thin ribbons (Figure S9c in the Supporting Information). The results imply that the gel state as the starting point of the crystallization process plays a key role in forming the crystalline structures with long-range order. FF gel networks may function as a confined matrix,[20] slowing down crystallization and promoting the kinetic adjustment, which thus leads to formation of crystalline structures with long-range order.

The thermal properties of as-prepared crystalline platelets and self-assembling fibrils before crystallization were studied by thermogravimetric analysis (TGA, Figure 2a). According to the TGA thermograms, there is a slight weight loss of the

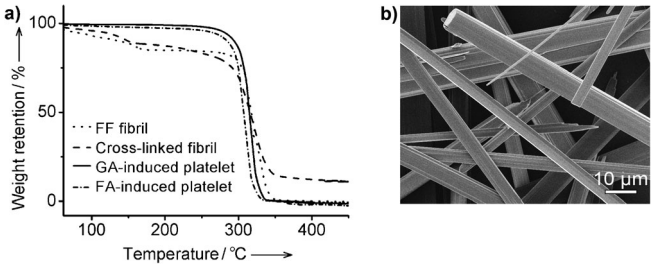

Figure 2. a) TGA curves of FF fibrils, cross-linked fibrils, formaldehyde (FA)-induced platelets, and GA-induced platelets. b) SEM image of platelets after thermal treatment at 200 °C.

FF fibrils and the cross-linked fibrils near 170 °C, which may be attributed to the release of phenylalanine in such self-assembling fibril structures.[21] The thermal decomposition of individual FF fibrils was completed at around 340 °C. At the same temperature, however, there is approximately 15 wt % residue left in cross-linked fibrils, attributable to the formation of some aldehyde-crossed FF derivatives having higher decomposition temperature. By contrast, the as-prepared crystalline platelets exhibit a single total weight loss at 340 °C, corresponding to complete thermal decomposition of the cyclo-Phe-Phe peptide. There is no indication of phenylalanine release in the process of thermal decomposition of platelets. This obvious difference in TGA thermograms before and after crystallization is considered to be the result of the change of peptide molecular structure. The crystalline platelets composed of diketopiperazine cyclo-Phe-Phe dipeptide have considerable thermal stability and maintain the structural integrity up to 200 °C. The thermal stability was also verified by direct observation of the crystalline platelets subject to thermal treatment at high temperature (200 °C). As shown in Figure 2b, no obvious structural deformation or defect resulted. Such thermal stability is extremely remarkable for a biological molecule and desirable for technological use.

The long-range oriented crystallization leads to the production of 3D crystalline peptide platelets capable of functioning as optical waveguides, a physical property newly emerging from small biologically derived molecules. Owing to the structural simplicity and tunability, functional versatility, ease of synthesis, and biocompatibility and biodegradation of small peptide building blocks, this physical property is increasingly important for application of biological or bioinspired materials with photonic and electric function in biomedical fields. As compared with the previously reported organic[21] and inorganic[9] waveguiding materials, the present peptide waveguide will surely extend its potential for application in biomedical fields, which require optical components to interface directly with living cells or systems.[10] Furthermore, peptide waveguides will naturally degrade and not leave any trace after they have acted as an optical element. Therefore, such functional structures of materials fabricated through self-assembly of versatile peptide molecules are advantageous in guiding light for biologically based modulation and sensing. A PL micrograph of peptide crystalline platelets is shown in Figure 3a. All platelets exhibited blue PL emission under excitation at 330–380 nm. There are remarkably bright PL spots at both ends, while comparatively weaker emission emanates from the platelet body (Figure 3b). This is a typical characteristic of an optical waveguide[11,22] and suggests that crystalline peptide platelets with long-range order can act as optical waveguide materials that absorb excitation light and then propagate emission light towards both ends. As observed from SEM images (Fig-

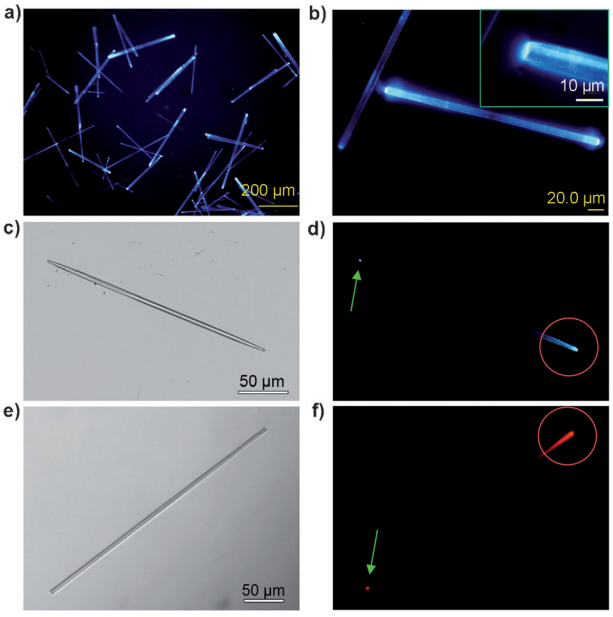

Figure 3. Optical waveguiding of peptide crystals. a) PL image of platelets excited at 330–380 nm. b) PL image of a single platelet showing brighter PL emission at the ends than in the body; the inset shows the PL of one end magnified. c–f) Direct observation of waveguiding with local excitation at one end of an individual platelet (c,d) and of a platelet incorporating NR dye (e,f). Note: (c) and (e) are bright-field images; (d) and (f) are PL images. The red circle marks the excitation area, and the green arrow denotes the out-coupling of PL emission at the other end.

ure 1a), there is no excessive peptide material at the bright PL ends instead of the presence of well-cleaved end facets, which indicates that the brighter spots at the ends result from guidance of light inside the platelets to their ends. Waveguiding was further confirmed by focusing the excitation light on one end of a platelet. Clearly, the guided PL was emitted from the other end (arrow in Figure 3d), whereas without waveguiding the PL emission should merely be observed at the local area of the excitation position. Such an outcoupling effect at an end is typical for waveguiding, and these peptide crystals can be classified as active waveguides,[22] because the guided light is generated within peptide platelets as a result of the inherent PL of cyclo-Phe-Phe dipeptide.[23] This finding implies that a peptide crystal with long-range order can function as an optical microcavity, thus allowing for propagation of PL emission along the longitudinal axis. PL emission of peptide crystals is readily tuned by simply incorporating guest dyes during crystallization. For instance, the incorporation of fluorescent Nile Red (NR) into peptide platelets leads to red emission upon excitation at 515–560 nm. As shown in Figure 3f, the emitted red PL can propagate along the platelet and be coupled out at the other end when one end of the platelet was excited. Scanning near-field optical microscopy (SNOM, Figure 4) reveals optical propagation losses within the peptide crystalline platelet arising from direct contact between the substrate and a facet of the platelet as well as Rayleigh scattering on account of compositional inhomogeneities and structural defects.[22]

In summary, we have reported hierarchically oriented crystallization upon introduction of an aldehyde in self-assembling fibrous peptide networks. The Schiff's base formed between the aldehyde and amino groups of the dipeptides plays a crucial role in triggering the intramolecular cyclization of linear dipeptides. The production and concomitant crystallization of cyclic dipeptides by digestion of the linear dipeptides initiates the phase transition from gel network structures to crystals. The overall stability of the crystalline structure is guaranteed by a cooperation of hydrogen bonding and π-stacking interactions. The crystalline platelets are uniaxially oriented along the longitudinal axis but with 3D ordered organization. We postulate that kinetic regulation is necessary for the confinement of ordered substructures in the crystals. These are extensively observed in nature where similar crystalline bundles or arrays are created naturally or by induction with external stimuli. Such peptide crystals with defined spatial dimensions exhibit remarkable thermal stability and optical waveguiding. This finding may open up a new avenue to design and develop optical or electrical materials and devices from biomimetic or bioinspired materials comprised of small biological molecules.

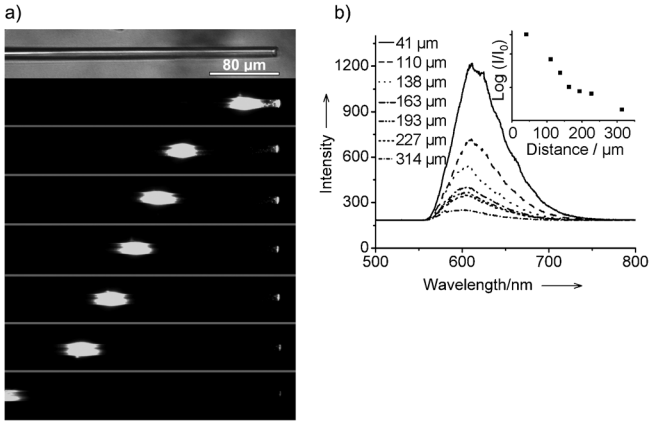

Figure 4. Propagation loss of the peptide crystal measured by SNOM. a) Bright-field optical image and PL images of a single peptide platelet showing the waveguide upon laser excitation at different positions. The bright spots indicate the laser excitation, the small spots on the right show the outcoupled light. b) Spatially resolved PL spectra of waveguided emission outcoupled at the end of the platelet in (a). Inset shows $\mathrm{Log}(I/I_0)$ versus distance between excitation and outcoupling for the PL spectra. The non-exponential decay indicates at least two different loss mechanisms; the decay length is about 200 micrometers.

Received: June 9, 2011
Published online: September 29, 2011

Keywords: fibers · peptides · optical waveguides · oriented crystallization · self-assembly

[1] S. W. Lee, C. B. Mao, C. E. Flynn, A. M. Belcher, *Science* **2002**, *296*, 892–895.
[2] H. J. Liang, G. Whited, C. Nguyen, G. D. Stucky, *Proc. Natl. Acad. Sci. USA* **2007**, *104*, 8212–8217.
[3] N. L. Nerurkar, B. M. Baker, S. Sen, E. E. Wible, D. M. Elliott, R. L. Mauck, *Nat. Mater.* **2009**, *8*, 986–992.
[4] L. R. Otterbein, P. Graceffa, R. Dominguez, *Science* **2001**, *293*, 708–711.
[5] a) K. Ariga, J. P. Hill, M. V. Lee, A. Vinu, R. Charvet, S. Acharya, *Sci. Technol. Adv. Mater.* **2008**, *9*, 014109; b) S. G. Zhang, *Nat. Biotechnol.* **2003**, *21*, 1171–1178; c) J. Aizenberg, P. Fratzl, *Adv. Mater.* **2009**, *21*, 387–388; d) S. Mann, *Nat. Mater.* **2009**, *8*, 781–793; e) I. Weissbuch, R. A. Illos, G. Bolbach, M. Lahav, *Acc. Chem. Res.* **2009**, *42*, 1128–1140.
[6] a) X. H. Yan, P. L. Zhu, J. B. Li, *Chem. Soc. Rev.* **2010**, *39*, 1877–1890; b) R. V. Ulijn, D. N. Woolfson, *Chem. Soc. Rev.* **2010**, *39*, 3349–3350, and references therein; c) L. Adler-Abramovich, D. Aronov, P. Beker, M. Yevnin, S. Stempler, L. Buzhansky, G. Rosenman, E. Gazit, *Nat. Nanotechnol.* **2009**, *4*, 849–854.
[7] T. Gädt, N. S. Ieong, G. Cambridge, M. A. Winnik, I. Manners, *Nat. Mater.* **2009**, *8*, 144–150.
[8] H. G. Cui, E. T. Pashuck, Y. S. Velichko, S. J. Weigand, A. G. Cheetham, C. J. Newcomb, S. I. Stupp, *Science* **2010**, *327*, 555–559.
[9] M. Law, D. J. Sirbuly, J. C. Jonhson, J. Goldberger, R. G. Saykally, P. Yang, *Science* **2004**, *305*, 1269–1273.
[10] S. T. Parker, P. Domachuk, J. Amsden, J. Bressner, J. A. Lewis, D. L. Kaplan, F. G. Omenetto, *Adv. Mater.* **2009**, *21*, 1–5.
[11] D. O'Carroll, I. Lieberwirth, G. Redmond, *Nat. Nanotechnol.* **2007**, *2*, 180–184.
[12] Y. S. Zhao, P. Zhan, J. Kim, C. Sun, J. X. Huang, *ACS Nano* **2010**, *4*, 1630–1636.
[13] M. Reches, E. Gazit, *Science* **2003**, *300*, 625–627.
[14] X. H. Yan, Y. Cui, Q. He, K. W. Wang, J. B. Li, *Chem. Mater.* **2008**, *20*, 1522–1526.
[15] a) P. M. Fischer, *J. Pept. Sci.* **2003**, *9*, 9–35; b) C. J. Dinsmore, D. C. Bashore, *Tetrahedron* **2002**, *58*, 3297–3312; c) A. K. Szardenings, T. S. Burkoth, H. H. Lu, D. W. Tien, D. A. Campbell, *Tetrahedron* **1997**, *53*, 6573–6593.
[16] A. Barth, C. Zscherp, *Q. Rev. Biophys.* **2002**, *35*, 369–430.

[17] K. E. van Holde, C. Johnson, P. S. Ho, *Principles of Physical Biochemistry*, 1st ed., Prentice Hall, Upper Saddle River, NJ, **1998**.
[18] K. Balakrishnan, A. Datar, R. Oitker, H. Chen, J. M. Zuo, L. Zang, *J. Am. Chem. Soc.* **2005**, *127*, 10496 – 10497.
[19] H. Cölfen, S. Mann, *Angew. Chem.* **2003**, *115*, 2452 – 2468; *Angew. Chem. Int. Ed.* **2003**, *42*, 2350 – 2365.
[20] J. A. Foster, M. M. Piepenbrock, G. O. Lloyd, N. larke, J. A. K. Howard, J. W. Steed, *Nat. Chem.* **2010**, *2*, 1037 – 1043.
[21] V. L. Sedman, L. Adler-Abramovich, S. Allen, E. Gazit, S. J. B. Tendler, *J. Am. Chem. Soc.* **2006**, *128*, 6903 – 6908.
[22] a) Y. S. Zhao, J. Xu, A. Peng, H. B. Fu, Y. Ma, L. Jiang, J. N. Yao, *Angew. Chem.* **2008**, *120*, 7411 – 7415; *Angew. Chem. Int. Ed.* **2008**, *47*, 7301 – 7305; b) D. O'Carroll, I. Lieberwirth, G. Redmond, *Small* **2007**, *3*, 1178 – 1183.
[23] N. Amdursky, M. Molotskii, D. Aronov, L. Adler-Abramovich, E. Gazit, G. Rosenman, *Nano Lett.* **2009**, *9*, 3111 – 3115.

